BNL-103705-2014-TECH

AGS/RHIC/SN 080;BNL-103705-2014-IR

Superconducting Helical Snake Magnets: Construction and Measurements

W. W. MacKay

August 1999

Collider Accelerator Department

Brookhaven National Laboratory

U.S. Department of Energy

USDOE Office of Science (SC)

DISCLAIMER

AGS/RHIC/SN #80

Superconducting Helical Snake Magnets: Construction and Measurements[1]

W. W. MacKay[a], M. Anerella[a], E. Courant,[a], J. Escallier[a], W. Fischer[a], G. Ganetis[a], A. Ghosh[a], R. Gupta[a], A. Jain[a], E. Kelly[a], A. Luccio[a], A. Marone[a], G. Morgan[a], J. Muratore[a], M. Okamura[b], V. Ptitsin[a], A. Prodell[a], T. Roser[a], S. Tepikian[a], M. Syphers[c], P. Wanderer[a], and E. Willen[a]

[a] BNL, Upton, NY
[b] RIKEN, Japan
[c] FNAL, Batavia IL

Abstract: In order to collide polarized protons, the RHIC project will have two snakes in each ring and four rotators around each of two interaction regions. Two snakes on opposite sides of each ring can minimize depolarization during acceleration by keeping the spin tune at a half. Since the spin direction is normally along the vertical direction in a flat ring, spin rotators must be used around an interaction point to have longitudinal polarization in a collider experiment. Each snake or rotator will be composed of four helical dipoles to provide the required rotation of spin with minimal transverse orbit excursions in a compact length of 10m. The basic helical dipole is a superconducting magnet producing a transverse dipole field which is twisted about the magnet axis through 360° in a length of 2.4 m. The design and construction of the magnets is described in this paper.

1 Introduction

For a helical dipole magnet with a twist wavelength of λ, the transverse magnetic field components in cylindrical coordinates may be expanded in terms of multipole coefficients ($\tilde{b}_n$ and $\tilde{a}_n$ for normal and skew components, respectively) as

$$B_r = B_0 \sum_{n=0}^{\infty} \frac{2^{n+1}(n+1)!}{(n+1)^{n+1}} \frac{1}{(kr_0)^n} I'_{n+1}\big((n+1)kr\big) \times \left[\tilde{a}_n \cos\left((n+1)\tilde{\theta}\right) + \tilde{b}_n \sin\left((n+1)\tilde{\theta}\right)\right] \tag{1}$$

$$B_\theta = B_0 \sum_{n=0}^{\infty} \frac{2^{n+1}(n+1)!}{(n+1)^{n+1}} \frac{1}{(kr_0)^n} \frac{I_{n+1}\big((n+1)kr\big)}{kr} \times \left[\tilde{b}_n \cos\left((n+1)\tilde{\theta}\right) - \tilde{a}_n \sin\left((n+1)\tilde{\theta}\right)\right], \tag{2}$$

[1]Work performed under the auspices of U. S. Department of Energy and RIKEN.

where I_n is the modified Bessel function, $k = 2\pi/\lambda$, and $\tilde{\theta} = \theta - kz$. Here z is measured down the axis, and θ is the polar angle relative to the horizontal plane. Off axis there is also a small longitudinal component of field. For the lowest order multipole contribution the field may be written as

$$B_x \simeq -B_0 \left\{ \left[1 + \frac{k^2}{8}(3x^2 + y^2) \right] \sin kz - \frac{k^2}{4} xy \cos kz \right\} \tag{3}$$

$$B_y \simeq B_0 \left\{ \left[1 + \frac{k^2}{8}(x^2 + 3y^2) \right] \cos kz - \frac{k^2}{4} xy \sin kz \right\} \tag{4}$$

$$B_z \simeq -B_0 k \left\{ 1 + \frac{k^2}{8}(x^2 + y^2) \right\} \left[x \cos kz + y \sin kz \right]. \tag{5}$$

Notice that there is an intrinsic sextupole component due to the helical twist of the magnet.

For an ideal helical magnet with a complete 360° rotation of the field about its axis, the integral of the transverse field components should be zero,

$$\int_0^\lambda \vec{B}_\perp \, dz = 0. \tag{6}$$

In this case it is easy to see that a particle entering the magnet along the magnet's axis will exit the magnet parallel to the axis but with a transverse displacement. Using this feature a snake has been designed by using two pairs (inner pair and outer pair) of right-hand-twisted helical dipoles of equal but opposite strength. Figure 1 shows the components of magnetic field (a), trajectory (c), and spin motion (e) for a particle propagated through the snake. When the two strengths (currents) are correctly set, a vertical spin will be flipped 180° about a rotation axis in the horizontal plane. By using two snakes on opposite sides of the accelerator and having rotation axes 90° apart in the horizontal plane, the spin tune can be kept at a half-integer as the beam is accelerated.

In a similar manner, a rotator can be made from four helices: two left-handed and two right-handed (Fig. 1b, d, and f).

2 Design

A cross section of the helical magnet is shown in Fig. 2a. The coil structure consists of two concentric aluminum tubes with slots that are filled with Kapton-insulated superconducting cable. The tubes are surrounded by a yoke made of single piece, low-carbon steel laminations. Holes near the outer perimeter of the yoke allow for tie rods, warm-up heaters, passage of helium coolant, and buss work for magnet interconnections. The winding slots rotate along the magnet length, but the holes in the yoke do not; these were therefore designed with rotational symmetry in mind. Azimuthal Lorentz forces are contained in the individual slots and, in contrast to the case of $\cos\theta$-dipole magnets made with keystoned cable, do not build up on the midplane turns. Along the length of the magnet, the outward Lorentz forces are ultimately contained by the single piece yoke. In the ends, the difficult Lorentz force problem is again solved by containing the forces in the individual slots, as shown in Fig. 2b. This figure also shows the reliefs machined into the tubes for the leads.

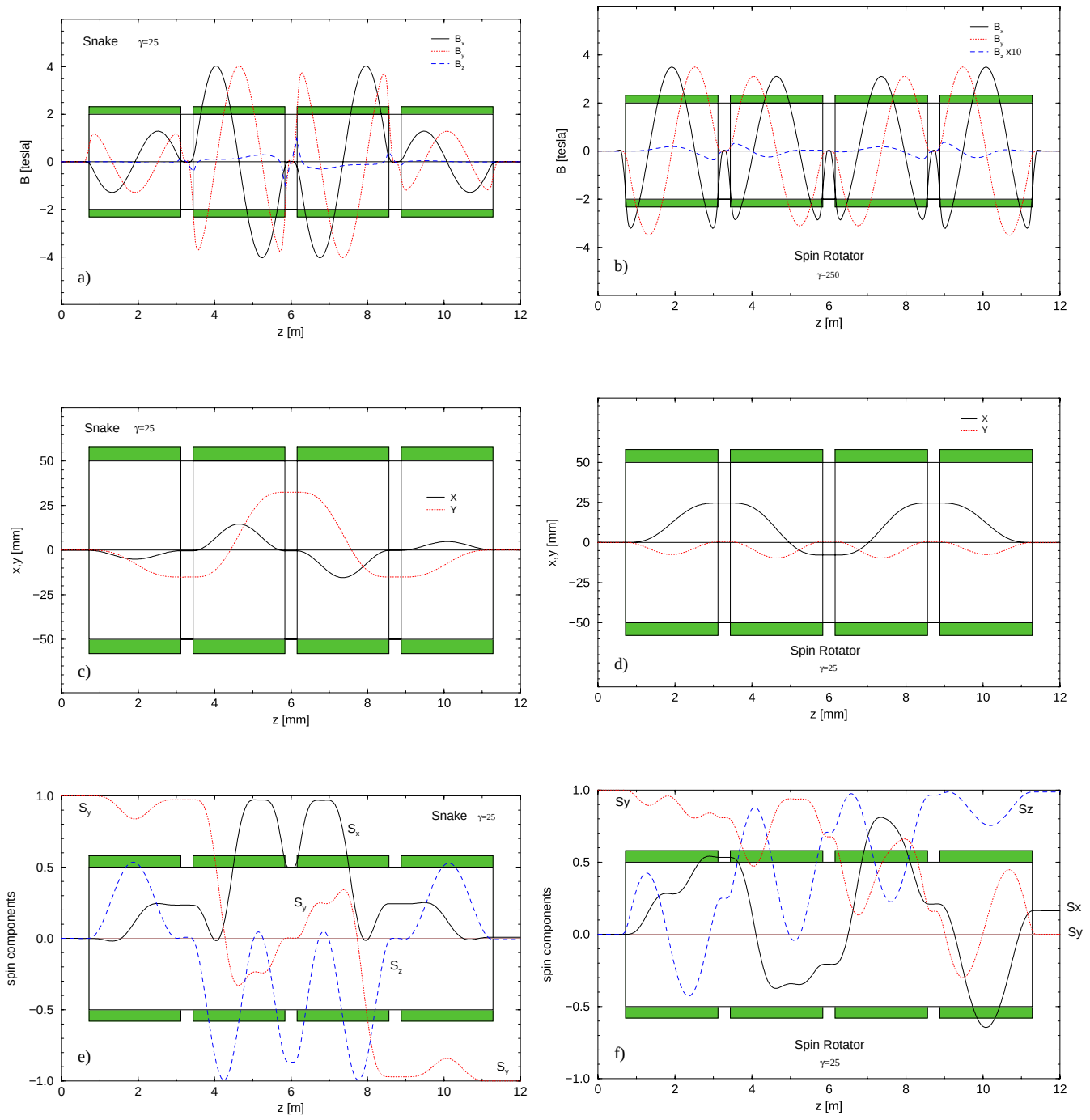

Figure 1: Field components plotted through a snake (a) and rotator (b); design injection trajectories through a snake (c) and rotator (d); spin precession through a snake (e) and rotator (f). The snake is constructed of four right-handed helices with vertical fields at the ends. The rotator is constructed of alternating right and left-handed helices with horizontal fields at the ends. In both the snake and rotator the inner two helices are wired in series, and the outer two helices are wired in series.

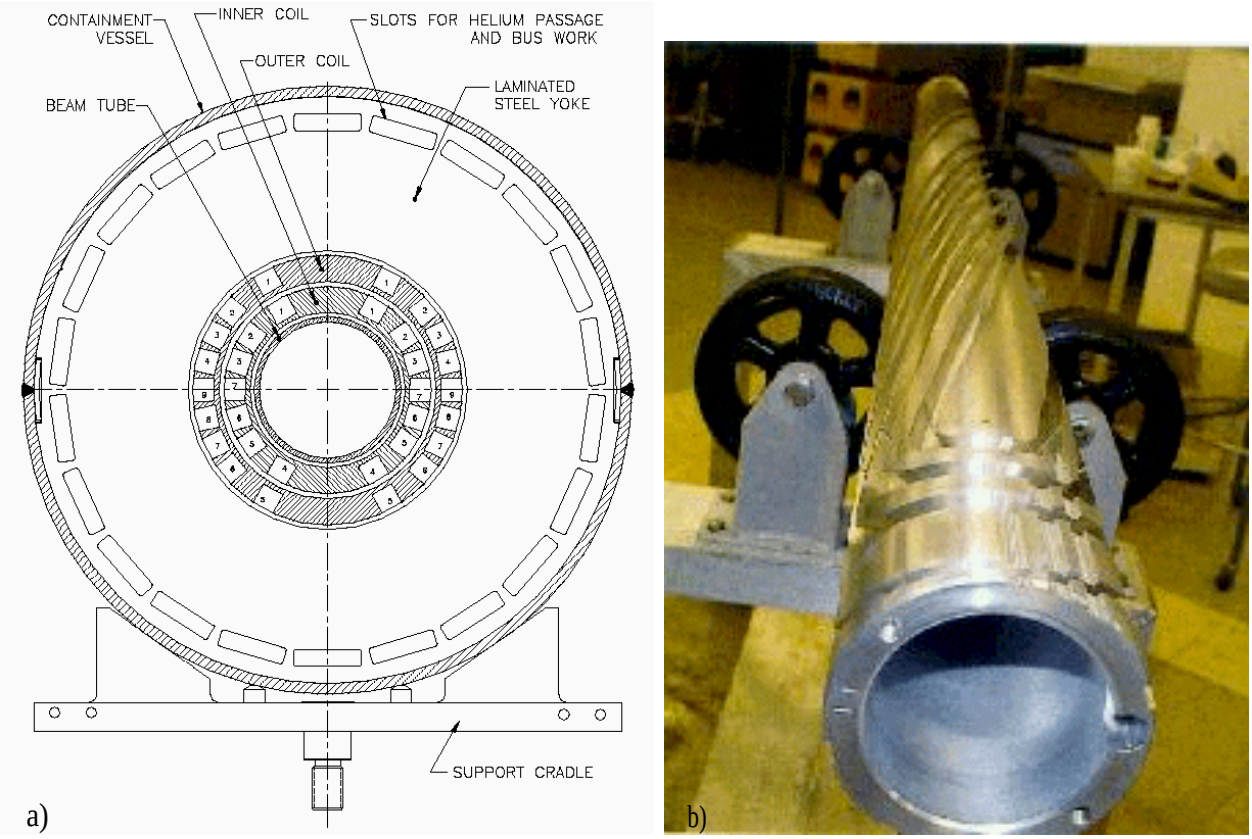

Figure 2: a) Cross section of a helical dipole. There are two layers of helical windings: 7 blocks in inner and 9 blocks in outer. b) A machined aluminum tube showing helical slots for the coil windings.

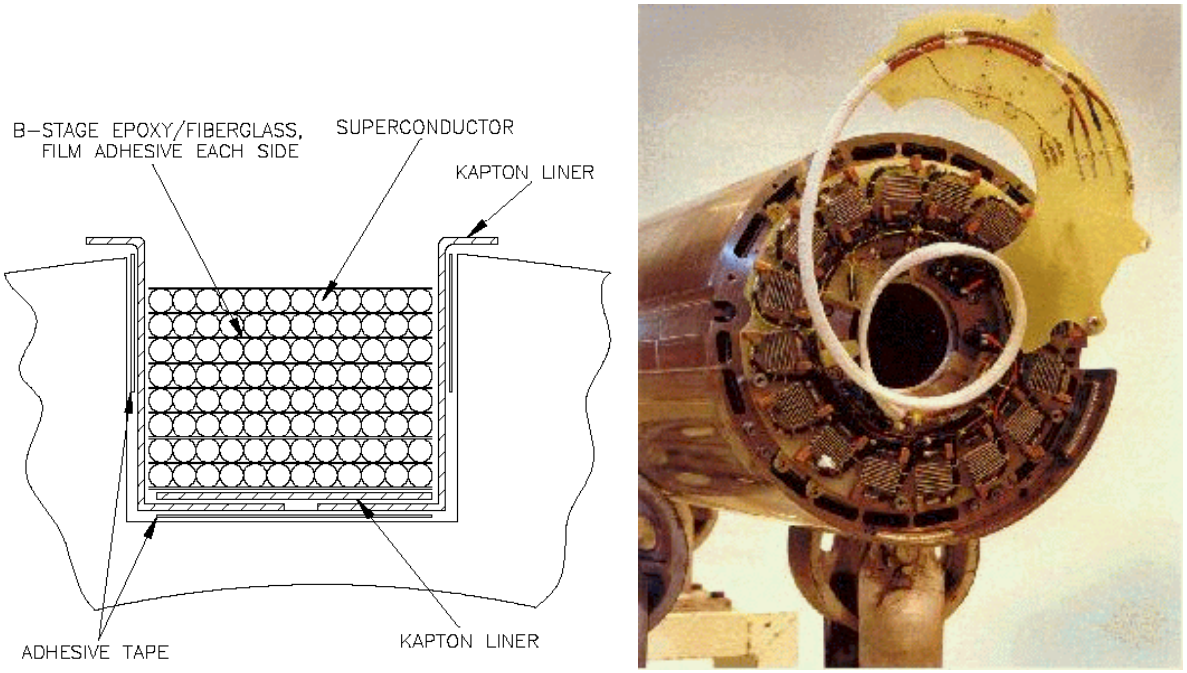

Figure 3: Left (a): Detailed cross section of one block of windings. Right (b): The lead end of a completed magnet showing the quench resistors and compact wiring harness. Since the separation between magnets is about 10 cm, the leads are attached to a pivoting plate for ease in wiring.

3 Construction

In order to wind the helical coils, we have the slots in the aluminum tubes (Fig. 2b) machined on a computer controlled milling machine. Each slot (Fig. 3a) is first lined with Kapton to minimize the chance of shorts to ground.

The superconducting cable is made of 7 wires twisted in a 6-around-1 pattern with a bare diameter of 0.99mm. After a double layer of Kapton insulation the diameter is 1.09mm. The critical current of the cable is about 476 A at 5 T and 4.2 K. The individual wires are made of 10μm diameter filaments of Niobium-Titanium superconductor inside a copper matrix to give a copper-to-superconductor ratio of 2.5:1.

The slots are hand wound with no tension in layers of 12 turns. A layer of B-stage Epoxy/Fiberglass with a double-sticky coating is placed under each layer to hold windings in place.

After winding, G10 fiberglass plates are applied to each slot and secured with ring clamps. A wrap of Kevlar 29 is applied to the tube to apply pressure to the G10 plates. The coils are then heat treated to allow the G10 plates to move inward while the B-Stage Epoxy fills the voids around the conductors. The stretch in the Kevlar winding keeps the plates under tension as the curing proceeds. After curing, the Kevlar is removed in order to dress and secure the leads with more epoxy. Before winding a new layer of Kevlar, a layer of fiberglass cloth is wrapped around the cylinder to cover sharp edges which might cut through the Kevlar. A dry layer of Kevlar is then wrapped around the cylinder. Next, a layer of Tedlar tape is wrapped to keep the Kevlar layer dry. Finally, fiberglass tape with wet epoxy is wound to bring the outer diameter of the cylinder slightly beyond the desired size. The cylinder is again heat treated to set the epoxy, and then machined to the required diameter.

The aluminum cylinders have been machined with holes and locating pins in one end to key them into a common base plate, thus ensuring that the inner and outer coil blocks are properly aligned. Since the cylinders separately constrain any magnetic forces, it is possible to leave a small amount of clearance so that the inner cylinder may be inserted into the outer cylinder without interference. The two cylinders and base plate are assembled with the leads sticking through holes in the base plate. The cylinders are then lowered into a stacking fixture (See Fig. 4a.) with the base plate pointing downward. One inch thick stacks of iron laminations are placed on the fixture and then lowered onto the coil cylinders. The fixture has three spring loaded hooks which hold the lamination stack perpendicular to the cylinders so that they do not bind as they are lowered. When the laminations reach the bottom, the hooks are pushed apart by the previous set of laminations leaving the new laminations in position as a counterweight raises the lamination holder.

Next the stacked magnet is removed from the stacking fixture, and the lead end is wired up. A 50mΩ resistor is connected across each of the 16 coil blocks to protect the windings during quenches. Each helical dipole will be cold tested in a vertical dewar. Measurements will be described in the next section.

Figure 4b shows the first of magnets on an alignment table which is used to assemble the completed cold mass of a snake (or rotator).

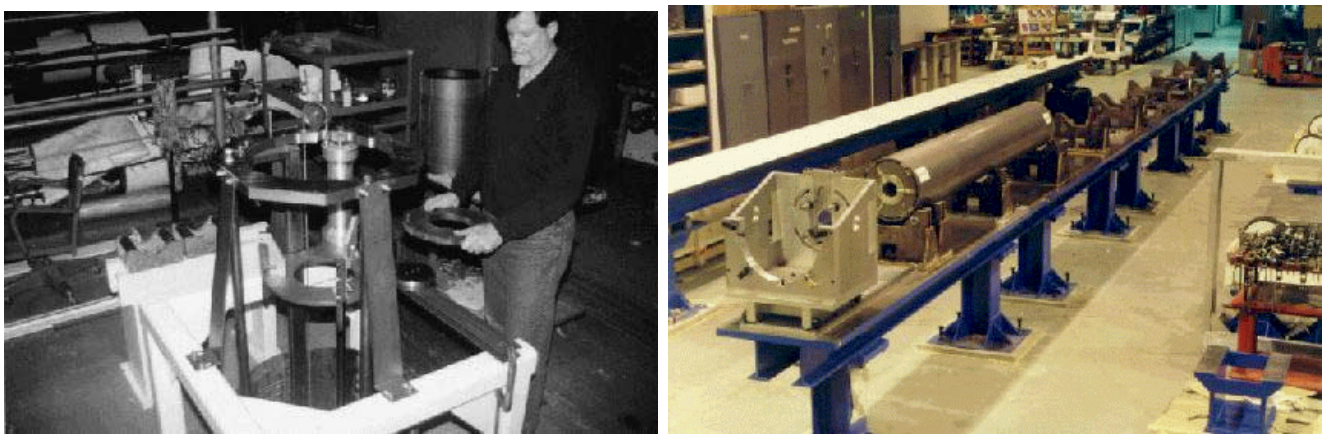

Figure 4: Left (a): Lamination stacking fixture. Right (b): Alignment table for assembling the cold mass of a complete snake or rotator. The first helical dipole is shown at the near end.

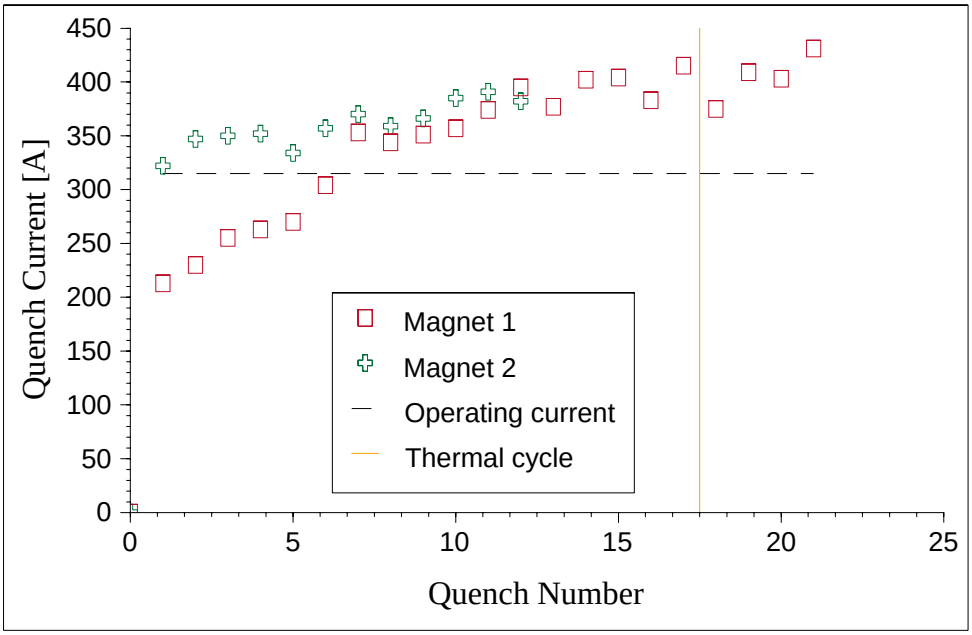

Figure 5: The quench training behavior for the first two magnets.

4 Measurements and Discussion

A series of measurements are made at various stages during the construction of the helical dipoles. Warm measurements of the coil resistance and high voltage standoff capability are made after the coils are wound, after the first and second curing, after the machining of the cylinders and after lamination stacking. These allow us to track problems in the manufacturing process and allow any needed repairs to be made before proceeding to the next step.

After the blocks are wired together, but before the quench resistors are installed, the field is measured at low current with a rotating coil to determine that the blocks have been wired correctly in series.

For field measurements, the magnet is hung in the vertical cryostat and cooled down to 4.2 K. The magnet is then ramped up in current until it quenches. This process is repeated until the magnet exceeds the operating current by a comfortable margin. (See Fig. 5.)

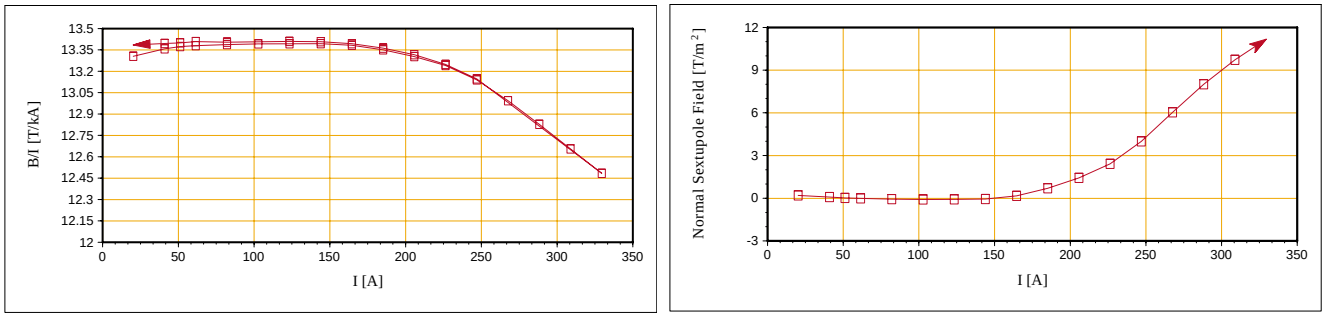

Figure 6: Measured transfer function (left) and sextupole field (right) as a function of current at the center of a single helical magnet.

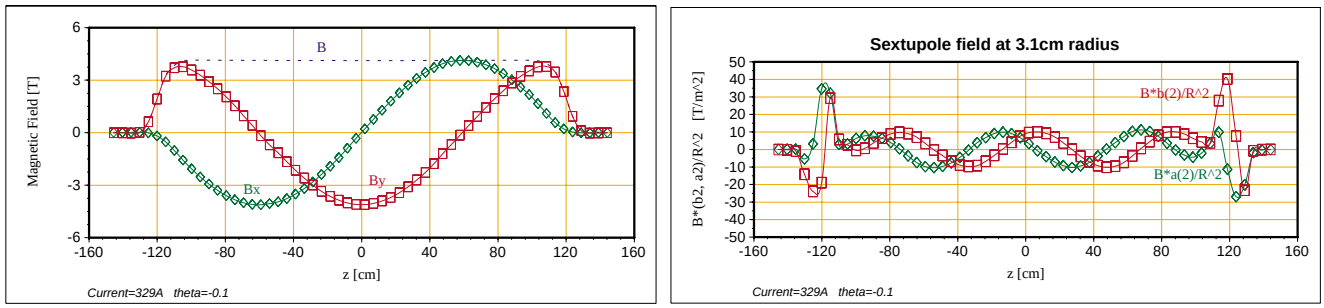

Figure 7: Measured dipole (left) and sextupole (right) components as a function of position along a single helical magnet.

The integral field as defined by Eq. 6 along the magnet is measured with tangential rotating coils which extend past the ends of the magnet. The tolerance[3] for this error has been estimated to be 0.050 Tm. Typical measured values peak around 0.015 Tm or less.

For the other field measurements, a short measurement probe with 5 cm long windings has been built. This probe is built on a translating fixture which can be positioned anywhere along the axis of the magnet. A series of measurements along an up/down-ramp cycle has been made at the center of the magnet. The measured transfer function (B/I) is shown in left side of Figure 6 for an up-ramp/down-ramp cycle of a typical magnet.

The right side of Figure 6 shows the normal sextupole field as a function of current for the up-ramp. The helical sextupole component is the lowest allowed harmonic after the dipole component. The low field behavior shows that the geometry of the magnet is good. The rise in helical sextupole above 150 A is due to saturation in the iron yoke. Ideally we would like to have a larger yoke, but we were limited to a 14" (35.5cm) diameter lamination due to cryostat size. The peak value of $11\mathrm{T/m}^{-2}$ corresponds to a helical sextupole component $\tilde{b}_2 = 26 \times 10^{-4}$ measured at a reference radius of $r_0 = 3.1$cm. While this at first seems to be a large value, the allowed tolerance has been estimated to be $21\mathrm{T/m}^{-2}$.

The reason for this looser tolerance to higher multipoles may be understood by looking at the longitudinal profile of the transverse field as shown in Figure 7. The dipole component rotates one complete turn along the magnet, whereas the sextupole field component rotates three times along the length of the magnet; this may also be seen by looking at the coefficients of $\tilde{\theta}$ in Eqs. 1 and 2 for the sextupole components with $n = 2$. Higher order multipoles will have even faster rotations. Since the betatron wavelength is between 12 and 50 m in the snakes, this rapid rotation of multipoles averages out to a much smaller effect than in a flat dipole

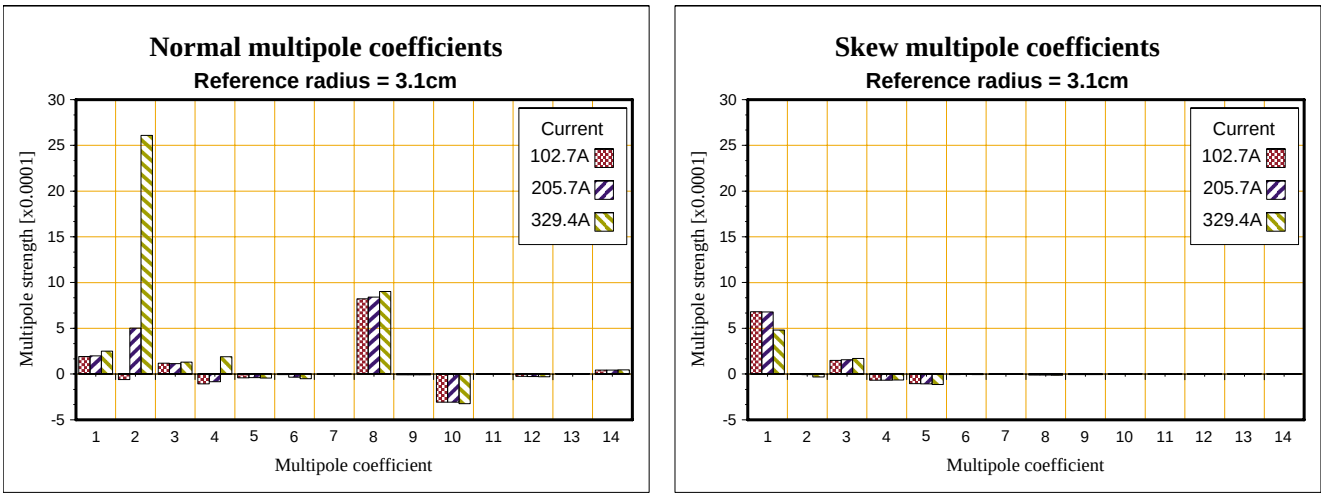

Figure 8: Measured multipole coefficients for three different currents measured at the center of the magnet. Only the normal sextupole and decapole components appear to show saturation effects.

bend with no rotation of field about the axis. Shifts in tune and chromaticity from this amount of sextupole appear to be small and quite manageable. Figure 8 shows the helical multipole coefficients in the body of the magnet at three different currents. The $n = 8$ components would rotate 9 times in the 2.4 m length of a single magnet, so 18-pole should produce very little effect on the orbit. Preliminary tracking with measured harmonics indicate that the addition of snakes and rotators should have a negligible effect on the dynamic aperture.

The measurements show that the design and construction of the magnets meet the specifications for a successful program.

5 Acknowledgements

We would like to thank Y. Shatunov for his help in the concept, and K. Hatanaka, T. Katayama, T. Kawaguchi, and T. Tominaka for their help in the formulation of the helical field equations. Of course, it must be stated that this would not have been possible without the fine craftsmanship of the technical team who actually built the magnets.

References

[1] E. Willen, et al., "Construction of Helical Magnets for RHIC", Proc. of 1999 Part. Accel. Conf., 3161 (1999).

[2] M. Syphers et al., "Helical Dipole Magnets for Polarized Protons in RHIC", Proc. of 1977 Part. Accel. Conf., 3359 (1998).

[3] I. Alekseev et al., "Design Manual Polarized Proton Collider at RHIC", (1998).